Effects of electrode chemical reactions on SF_6 discharge characteristics in extremely inhomogeneous electric fields

Zhicheng Wu, Qiaogen Zhang, Chaoqun Ma, and Heli Ni

Citation: Physics of Plasmas **25**, 072104 (2018); doi: 10.1063/1.5040402
View online: https://doi.org/10.1063/1.5040402
View Table of Contents: http://aip.scitation.org/toc/php/25/7
Published by the American Institute of Physics

Effects of electrode chemical reactions on SF_6 discharge characteristics in extremely inhomogeneous electric fields

Zhicheng Wu,[a] Qiaogen Zhang,[a] Chaoqun Ma,[a] and Heli Ni[a]
State Key Laboratory of Electrical Insulation and Power Equipment, Xi'an Jiaotong University, Xi'an 710049, China

(Received 17 May 2018; accepted 18 June 2018; published online 3 July 2018)

SF_6 is widely used in the gas-insulated metal-enclosed switchgear or the corona-stabilized gas spark switch applications as a gas dielectric. It is generally believed that the discharge characteristics are only related to the electric field distribution and gas molecular density; however, the electrode chemical reactions can indeed markedly affect the SF_6 discharge characteristics in the extremely inhomogeneous electric fields under the steady-state voltage. In this study, we used a needle-plane electrode system to build an extremely inhomogeneous electric field and examined the discharge characteristics within it including *U-p* characteristics, corona appearance, and corona current. We also analyzed the micro-region characteristics of the electrode surface, including the surface morphology, elemental composition, and chemical state to fully qualitatively determine the role of the electrode chemical reactions in discharge behavior. We found that the N-shaped *U-p* curve widens, the filamentous leader channels disappear, and the corona current drops suddenly as the duration of the electrode chemical reactions increases. Varying the surface morphology, elemental composition, and chemical state was observed on the electrodes of different polarities through micro-region analysis. The metal fluoride or metal sulfide film on the electrode surface may serve as a resistive coating due to its low electrical conductivity, which obstructs the leader discharge while enhancing the streamer discharge, suppressing the transition from the streamer to leader discharge and altogether significantly altering the discharge characteristics. The resistive coating produced is the primary cause of the electrode chemical reaction effects on the discharge characteristics, primarily as it depresses the transition from the streamer to leader discharge. The results presented here may provide useful guidelines for further research on SF_6 discharge under inhomogeneous electric fields. *Published by AIP Publishing*. https://doi.org/10.1063/1.5040402

I. INTRODUCTION

SF_6 is widely used in the gas-insulated metal-enclosed switchgear (GIS) and the corona-stabilized gas spark switch applications as a gas dielectric.[1–3] As far as the discharge characteristics in SF_6 under the uniform and inhomogeneous electric fields are concerned, with the high gas pressure they are particularly worth researching as the experimental condition must be fitted to the working conditions of GIS. It was once generally believed that the discharge characteristics were only related to the electric field distribution and gas molecular density; however, the by-products of SF_6 do markedly affect the discharge characteristics. Indeed, the changes in the discharge characteristics due to the SF_6 decomposition have been extensively studied in the recent years.[4,5] Our research team has long been dedicated to studying the discharge characteristics of SF_6 in various voltage waveforms.[6–8] We found that the electrode chemical reactions severely affect these characteristics in the extremely inhomogeneous electric fields under the steady-state voltage; further, this process affects the discharge characteristics within a short amount of time far beyond the effects of the SF_6 gas decomposition process.

To date, only one research group has studied the electrode chemical reactions that occur in the discharge of SF_6 gas. In 1986, Macgregor *et al.* performed SF_6 glow discharge and corona discharge with a gas pressure under 200 Torr and observed that the structure of the discharge changes over time.[9] They attributed this phenomenon to electrode-fluorine reactions. Nickel is recommended as an electrode material according to their results. However, their research lacked a truly detailed assessment of the discharge characteristics or the role of these reactions on discharge. This phenomenon merits further, more comprehensive research.

In this study, we used a needle-plane electrode system to build an extremely inhomogeneous electric field and examined its discharge characteristics including *U-p* characteristic, corona appearance, and corona current. We then analyzed the micro-region characteristics of the electrode surface, including surface morphology, elemental composition, and chemical state. We qualitatively determined the role of the electrode chemical reactions in the discharge. Our results show that the film produced by the electrode chemical reactions can depress the transition from the streamer discharge to the leader discharge. We hope that this paper represents a workable guideline for future research on SF_6 discharge under inhomogeneous electric fields.

II. EXPERIMENTAL PROCEDURES

We used a needle-plane electrode system to research the discharge characteristics of SF_6 in an extremely inhomogeneous

[a]Electronic addresses: z_c_wu@163.com, hvzhang@mail.xjtu.edu.cn, cqma123@stu.xjtu.edu.cn, and niheli_xjtu@yeah.net

electric field. The needle electrode is fabricated from nickel as a hemispherical-capped cylinder with a curvature radius of 500 μm. The plane electrode is made up of stainless steel and well chamfered. The gap distance was set to precisely 10 mm. The electric field of this electrode system was calculated by boundary element method. The uniformity coefficient f calculated in accordance with equation (1) is 15.2, so the electrode system produces a typical extremely inhomogeneous electric field (here E_{max} is maximum electric field strength, U is applied potential, and h is gap separation). The equipotential lines and electric field strength along the needle axis are shown in Fig. 1

$$f = E_{max} \Big/ \left(\frac{U}{h}\right). \tag{1}$$

The whole electrode system was placed in a sealed chamber to carry out the experiments across a wide gas pressure range. The experimental chamber was evacuated to vacuum (gas pressure < 60 Pa) and filled with commercial SF_6 (purity $> 99.997\%$) with a gas pressure between 0.1 MPa and 0.5 MPa.

A positive DC voltage was applied to the needle electrode, and then, the high voltage DC voltage was measured by a resistive divider with a voltage ratio of 9907:1.[10] The corona current was measured by a Techimp® clamp high frequency current transformer (HFCT) with a bandwidth (-6 dB) of 2 MHz to 60 MHz and sensitivity of 21 mV/mA. The integration image of corona discharge was captured by a SLR camera (Nikon® D300) with an exposure time of 2.5 s and photosensitivity of ISO-6400.

In order to characterize the surface of electrode after the electrode chemical reactions, we analyzed the micro-region characteristics, including surface morphology, elemental composition, and chemical state. The high resolution images of the needle electrode surface were collected on a scanning electron microscope (SEM) HITACHI® SU3500 at 15 kV. X-ray photoelectron spectroscopy (XPS) studies were carried out on a ThermoFisher® ESCALAB Xi$^+$ using an Al K α monochromated (100 eV pass energy, 500 μm spot size) source. The samples were etched by a low-energy Ar^+ flood source.

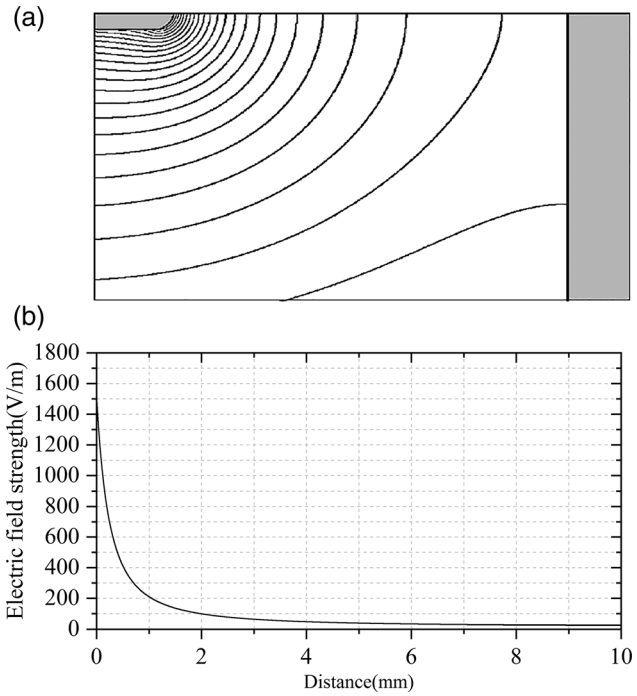

FIG. 1. Equipotential lines and electric field strength distribution along needle axis: (a) equipotential lines and (b) electric field strength distribution along needle axis (U = 1 V).

III. EFFECTS ON DISCHARGE CHARACTERISTICS

The effects of the electrode chemical reactions on the discharge characteristics are mainly embodied in the U-p characteristic, the corona appearance, and the corona current.

A. Effects on *U-p* characteristic

The U-p characteristic of SF_6 describes the relationship between the breakdown voltage of the gas gap and the gas pressure. It is useful to design a corona-stabilized gas spark switch or to monitor the condition of GIS, so it is often researched as an important part of the discharge characteristic. The U-p characteristic of SF_6, as opposed to that of air, has a non-monotonous trend at lower gas pressure due to its strong electronegativity.[8] The trend is non-monotonous due to the different pre-breakdown processes at different gas pressures. The breakdown mode changes from the streamer breakdown to the leader breakdown as the gas pressure increases. Once the leader channel appears, the breakdown voltage drops off due to the high conductivity of the leader channel, which forms an N-shaped U-p curve.

We pretreated the electrode system with a corona discharge with a gas pressure of 0.1 MPa and a positive DC voltage of 45 kV to research the effects of the electrode chemical reactions on U-p characteristics. After pretreatment, fresh SF_6 was applied in each subsequent experiment to eliminate the effects of the decomposition gas on the discharge. The U-p characteristics of the corona discharge in SF_6 after varying pre-treating time are shown in Fig. 2. The breakdown voltage

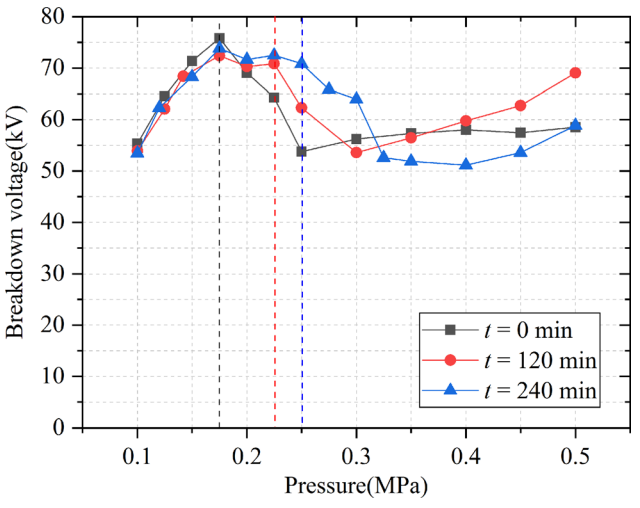

FIG. 2. U-p characteristic of different electrode chemical reaction durations. Reactions were carried out via corona discharge with gas pressure of 0.1 MPa and positive DC voltage of 45 kV. Note that breakdown voltage plunge increases as electro chemical reaction duration increases.

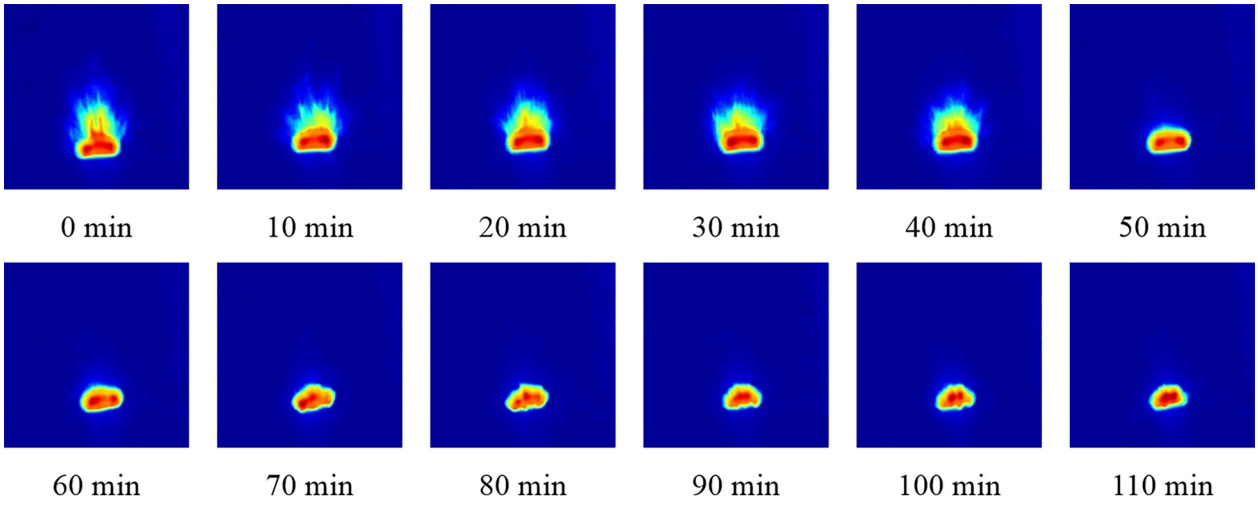

FIG. 3. Corona appearance with time as an independent variable. The experiment is carried out with a gas pressure of 0.25 MPa and a positive DC voltage of 45 kV. Note that the filamentous leader channels disappear suddenly after 50 min.

at the streamer breakdown gas pressure range was almost invariable before and after pretreatment, but the gas pressure at which the breakdown voltage plunge occurred was markedly affected. Before the pretreatment, this gas pressure was 0.175 MPa; after pretreatment with a duration of 120 min and 240 min, this pressure increased to 0.225 MPa and 0.25 MPa, respectively. The effects of the electrode chemical reaction merely widen the N-shaped *U-p* curve; that is, the breakdown voltage increases within a specific pressure range while the maximum value of the breakdown voltage does not significantly change. Per the N-shaped *U-p* curve, we can reasonably speculate that the electrode chemical reaction effectively suppressed the transition from the streamer discharge to the leader discharge and thus raised the gas pressure at which the breakdown voltage plunge occurs.

B. Effects on corona appearance

As discussed above, the depression of the transition from the streamer to leader charge appears to be the cause of changes in the *U-p* characteristics by the electrode chemical reactions. To verify this conjecture, we recorded the corona appearance at 0.25 MPa under 45 kV positive DC voltage with time as an independent variable as shown in Fig. 3. The experiment was carried out for 2 h until corona appearance remained stable. After 50 min of the experimentation, the filamentous discharge channels in front of the needle electrode disappeared suddenly, and a discharge with uniform brightness and symmetrical structure remained instead. Based on the theory established by Niemeyer, these bright and thick channels are leader channels.[11] Unlike from the discharge mode under impulse voltage, the leader channels may stably appear under the steady-state voltage without breakdown, so these strong discharges with the leader channels can be regarded as leader coronas. After these filamentous leader channels disappeared, a uniform optical region was caused by the streamer corona. In summary, the occurrence of the leader discharge is more difficult as the discharge time increases and the electrode chemical reactions which in turn affect the breakdown voltage determined by the leader discharge. This phenomenon also confirms the conjecture discussed above.

C. Effects on corona current

The phenomena discussed above support our conjecture from a quantitative perspective. We next measured the corona current by HFCT. The relationship between the corona current amplitude and discharge time is shown in Fig. 4. The value of the first peak of the current waveform was regarded here as the current pulse amplitude. The average corona current amplitude of the discharge within 1 min was used to rule out the randomness of the discharge. The experimental conditions were consistent with those described in Sec. III B.

According to Fig. 4, the corona discharge suddenly dropped about 50 min into the experiment. This phenomenon corresponds to the sudden disappearance of the leader corona described above. The leader corona occurrence was accompanied by a vigorous thermal ionization process, so the corona current was greater if there was a leader channel. The

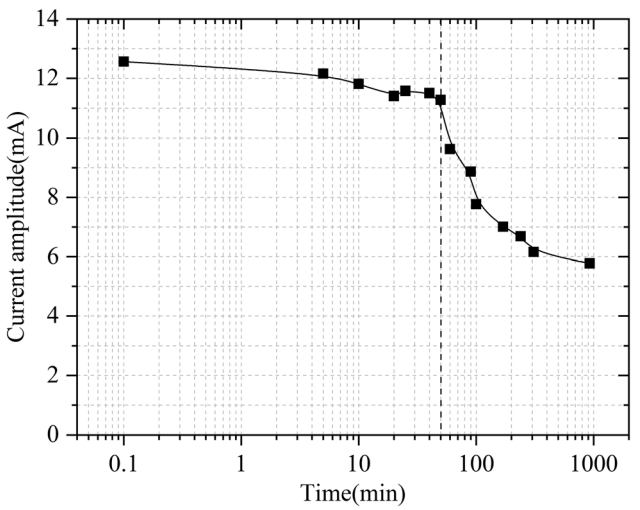

FIG. 4. Current amplitude of corona discharge as a function of experimental time. Same experimental conditions as shown in Fig. 3. Note that the corona current drops suddenly at 50 min.

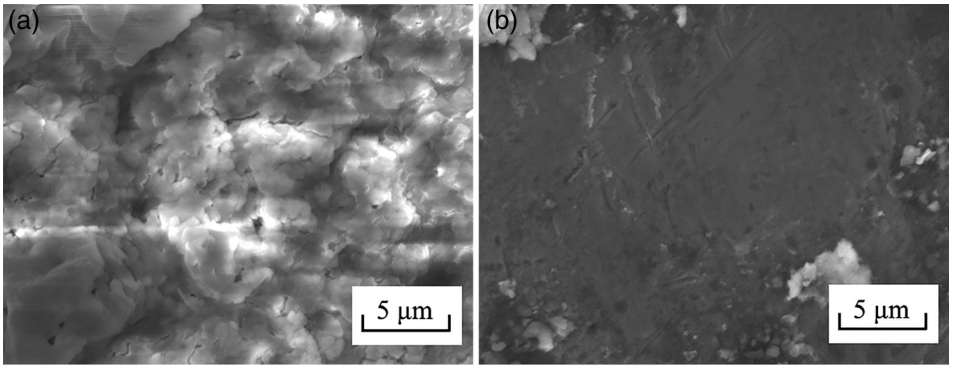

FIG. 5. SEM images of needle electrodes with varying polarity. Note that the coarse and fluffy positive needle electrode versus continuous and compact negative needle electrode, (a) Positive needle electrode surface, (b) Negative needle electrode surface.

leader corona did not form as easily as time progressed and after the electrode chemical reaction occurred, which decreased the current amplitude. The current amplitude stabilized to about 6 mA when only the steady streamer corona was present.

IV. MICRO-REGION ANALYSIS OF ELECTRODE SURFACE

The electrode chemical reaction produced a layer of film on the electrode surface which affected the transition from the streamer discharge to the leader discharge. The characteristics of this film reveal the role of the electrode chemical reactions in producing different discharge characteristics. The needle electrode is located in the high electric field strength region, so the effects of the chemical reactions on the surface of needle electrode are more significant in regard to the discharge characteristics; this section discusses only the needle electrode surface. We also analyzed the electrode chemical reactions of both polarities due to the notable polarity effect of the SF_6 discharge characteristics in an extremely inhomogeneous electric field. In this experiment, we pretreated the electrode system with a corona discharge with a gas pressure of 0.1 MPa and a positive DC voltage of 45 kV for a 60 min duration.

The surface morphologies of the needle electrodes of different polarities were observed by SEM as shown in Fig. 5. We found that the film on the positive needle electrode surface was coarse and fluffy and the film on the negative needle electrode was continuous and compact. Therefore, the electrode chemical reactions occurring on the different electrodes were different and produced markedly different surface morphologies.

We next used XPS for quantitative and qualitative analysis of the needle electrode surface within 5 nm thickness to characterize the elemental composition and chemical state of the film on the electrode surface. The elemental composition was obtained from the results of the full spectra scan. The mass fractions of the major element on the positive and negative needle electrode surface are shown in Fig. 6. Compared with the negative needle electrode surface, more F was detected on the surface of the positive surface electrode. The mass fraction of S is close to F at the positive needle electrode surface, but the mass fraction of F was only one third of S at the negative needle electrode surface. Oxidation and contamination were unavoidable during the preparation and transfer of samples, so more impurities such as C, O, and Si appeared on the surface.

We next qualitatively analyzed the possible reaction paths of F on the electrode surface. When the energetic electrons collide with SF_6 molecules, F^- may be formed as shown in (2). The F^- ions drift under the electric field and move to the surface of the positive needle electrode, where they react with the metal to produce metal fluoride. This is the first reaction path that generates metal fluorides, which is electric-dependence

$$e + SF_6 \rightarrow F^- + SF_5. \quad (2)$$

SF_6 is decomposed into low-fluorine sulfides such as SF_5 and SF_4 in the areas with high electric field strength.[4,12] These low-fluorine sulfides react with moisture to generate HF, which can strongly corrode metals and generate metal fluorides as shown in (3). In addition, SF_6 dissociation can occur under electron impacts, and therefore, dissociative fluorine atoms with high chemical reactivity should be reacted with electrode material as shown in (4) and (5). These are the second reaction paths to generate metal fluorides, which are electric-independence

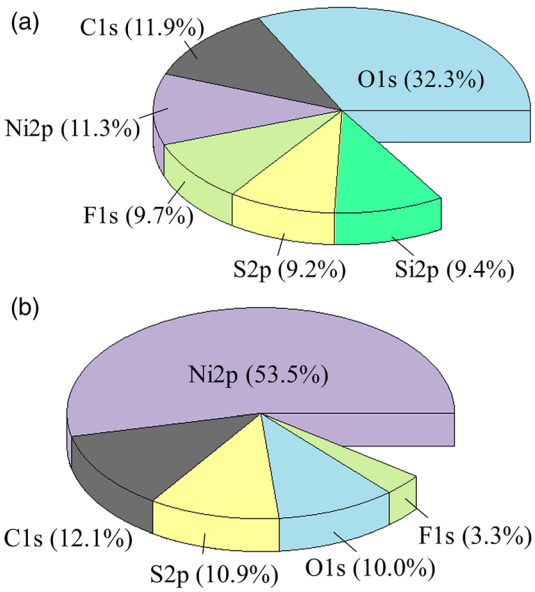

FIG. 6. Mass fractions of major element on the positive and negative needle electrode surfaces based on the XPS results, (a) Positive needle electrode surface, (b) Negative needle electrode surface.

$$Ni + 2HF \rightarrow NiF_2 + H_2, \quad (3)$$

$$e + SF_6 \rightarrow SF_5 + F + e, \quad (4)$$

$$Ni + 2F \rightarrow NiF_2. \quad (5)$$

The first and the second reaction paths occur simultaneously on the surface of the positive needle electrode. Only the second reaction path occurs on the surface of the negative needle electrode. Therefore, the mass fraction of F on the surface of the positive needle electrode is higher than that on the negative electrode surface.

We used XPS to characterize the chemical state of F and S. The high-resolution spectra of S 2p and F 1s are shown in Fig. 7. According to the spectra of S 2p on the surface of the positive needle electrode, the S 2p spectrum [Fig. 7(a)] was fitted by considering two resolved doublets (with a spin–orbit splitting of ∼1.16 eV between 2p3/2 and 2p1/2) located at 169.0 eV and 170.0 eV, which can be assigned to $NiSO_4$.[13] We obtained different results on the negative needle electrode, where the S 2p3/2 and 2p1/2 peaks [Fig. 7(b)] were observed at 162.2 and 163.39 eV, respectively. These results indicate different chemical states from the positive electrode surface, which can be assigned to NiS. The F 1s spectra of the positive and negative needle electrodes were observed on the main peak at 684 eV–685 eV [Figs. 7(c) and 7(d)], which is assigned to metal fluoride, i.e., NiF_2.[14] In summary, NiF_2 and $NiSO_4$ were present on the positive needle electrode while NiF_2 and NiS were present on the negative electrode needle electrode.

V. ROLE OF THE ELECTRODE CHEMICAL REACTION IN THE DISCHARGE CHARACTERISTICS

Per the above results, we believe that the electrode chemical reaction generates a layer of metal fluoride or metal sulfide film on the surface of the needle electrode. This section discusses the role of this film in the discharge process.

Consider nickel fluoride as an example. Its electrical conductivity is very low,[15] about $10^{13}\ \Omega\,m^{-1}$. Thus, this film can be regarded as a resistive coating. The resistive coating covers the bare electrode, so the discharge mode is changed. In our opinion, there exist two roles of this resistive coating.

The first role is a current-limiting resistance, which is equivalent to a resistor connected in series of the discharge circuit. The streamer channels that require less charge injection can be preserved, but the leader channels that require more charge injection are limited. The second role is a leakage circuit of interface charge; in this role, the resistive coating is equivalent to a series of parallel combinations of partial resistances and partial capacities as shown in Fig. 8.[16] In the positive needle electrode, negative charges are accumulated on the side of the resistive coating near the gas and negative charges reduce the electric field strength E_g on the gas side so that the subsequent discharges do not readily occur. The leakage of these negative charges, due to the existence of partial resistances, causes a rapid recovery of the electric field strength E_g and the rapid occurrence of the subsequent discharges. Frequent streamer discharges make the electric field distribution uniform in the gas gap, i.e., the corona stablization.[17]

In the synergistic effect of these two mechanisms, the leader discharge does not easily occur while the streamer discharges occur frequently, which suppresses the transition from streamer to the leader discharge and altogether significantly alters the discharge characteristics, including the *U-p* characteristics, the corona appearance, and the corona current.

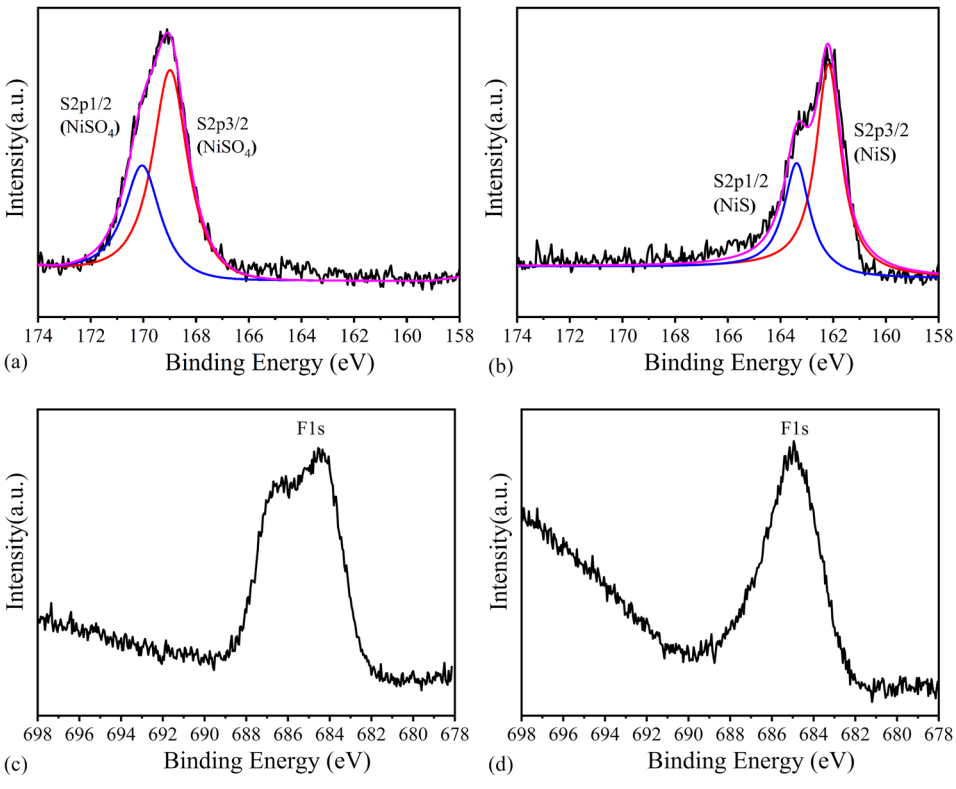

FIG. 7. XPS spectra of S 2p and F 1s with high resolution of the positive and negative electrode surfaces, (a) S 2p (positive), (b) S 2p (negative), (c) F 1s (positive), (d) F 1s (negative).

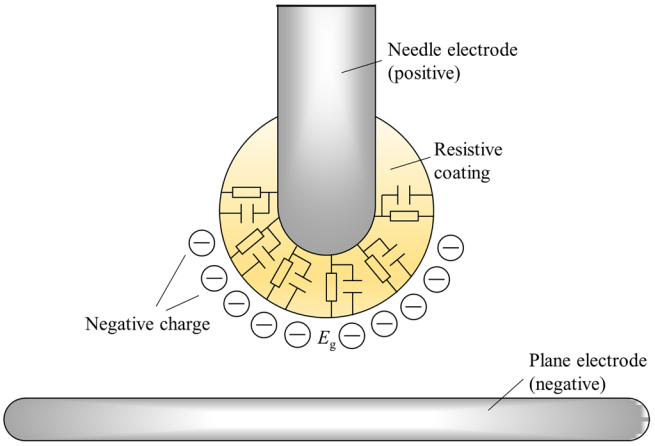

FIG. 8. Schematic of the equivalent circuit of the resistive coating.

VI. CONCLUSION

This paper discussed the detailed discharge characteristics in a needle-plane electrode system. We analyzed the micro-region characteristics of the electrode surface and qualitatively determined the role of the electrode chemical reactions in the discharge. Our results can be summarized as follows:

(1) We found that the discharge characteristics including the *U-p* characteristics, the corona appearance, and the corona current are influenced by the electrode chemical reactions. As the duration of the electrode chemical reactions increases, the N-shaped *U-p* curve widens, the filamentous leader channels disappear, and the corona current suddenly drops. These phenomena are caused by the suppression of the transition from the streamer to leader charge.

(2) Micro-region analysis of the electrode surface revealed the effects of the electrode chemical reactions on surface morphologies, elemental compositions, and chemical states. We found that the film on the positive needle electrode is coarse and fluffy and the film on the negative needle electrode is continuous and compact. Compared with the negative needle electrode surface, more F was detected on the surface of the positive surface electrode due to two different reaction paths. According to the high-resolution XPS spectra we gathered, NiF_2 and $NiSO_4$ are present on the positive needle electrode and NiF_2 and NiS are present on the negative needle electrode.

(3) Metal fluoride or metal sulfide film on the electrode surface can be regarded as a resistive coating due to its low electrical conductivity. This resistive coating plays two roles: first, as a current-limiting resistance and second, as a leakage circuit of interface charge. In the synergistic effect of these two mechanisms, the leader discharge does not readily occur while the streamer discharges occur frequently, which suppresses the transition from the streamer discharge to the leader discharge and altogether significantly alters the discharge characteristics.

[1]P. Osmokrovic, M. Vujisic, K. Stankovic, A. Vasic, and B. Loncar, Plasma Sources Sci. Technol. **16**, 643 (2007).
[2]H. Zhao, X. Li, S. Jia, and A. B. Murphy, J. Appl. Phys. **113**, 143301 (2013).
[3]J. A. Harrower, S. J. Macgregor, and F. A. Tuema, J. Phys.: Appl. Phys. **32**, 790 (1999).
[4]A. V. Phelps and R. J. Van Brunt, J. Appl. Phys. **64**, 4269 (1988).
[5]W. Ding, G. Li, X. Ren, X. Yan, F. Li, W. Zhou, and F. Wang, IEEE Trans. Dielectr. Electr. Insul. **22**, 3278 (2015).
[6]H. You, Q. Zhang, J. Ma, Y. Qin, T. Wen, C. Guo, and Y. Zhang, IEEE Trans. Dielectr. Electr. Insul. **23**, 2677 (2016).
[7]Z. Wu, Q. Zhang, J. Ma, X. Li, and T. Wen, "Effectiveness of on-site dielectric test of GIS equipment," IEEE Trans. Dielectr. Electr. Insul. (to be published).
[8]Z. Wu, Q. Zhang, J. Ma, Q. Du, L. Zhang, X. Li, C. Gao, and G. Wang, in *2017 IEEE Electrical Insulation Conference, Baltimore, USA, 11 June–14 June 2017*, pp. 66–69.
[9]S. J. Macgregor, G. A. Woolsey, D. B. Ogle, and O. Farish, IEEE Trans. Plasma Sci. **14**, 538–543 (1986).
[10]A. Kovacevic, D. Despotovic, Z. Rajovic, K. Stankovic, V. Kovacevic, and U. Kovacevic, Nucl. Technol. Radiat. **28**, 182 (2013).
[11]L. Niemeyer, L. Ullrich, and N. Wiegart, IEEE Trans. Electr. Insul. **24**, 309 (1989).
[12]T. M. Miller, A. E. S. Miller, J. F. Paulson, and X. Liu, J. Chem. Phys. **100**, 8841 (1994).
[13]R. B. Shalvoy and P. J. Reucroft, J. Vac. Sci. Technol. **16**, 567 (1979).
[14]B. P. Loechel and H. H. Strehblow, J. Electrochem. Soc. **131**, 713 (1984).
[15]J. Salardenne, M. Salagoïty, J. Pichon, and A. S. Barriere, Thin Solid Films **88**, 153 (1982).
[16]M. Laroussi and I. Alexeff, in *IEEE Conference on Pulsed Power Plasma Science, Las Vegas, USA, 17 June–22 June 2001*, p. 169.
[17]T. Hinterholzer and W. Boeck, in *IEEE Conference on Electrical Insulation and Dielectric Phenomena, Victoria, Canada, 15 October–18 October 2001*, pp. 413–416.